THE GLOBAL AND LOCAL LIMIT LOADS OF RPV WITH NOZZLE CORNER CRACK

Yuebing Li[1], Yang Liu[2]

[1] Professor, College of Mechanical Engineering, Zhejiang University of Technology, Hangzhou, China (ybli@zjut.edu.cn)
[2] Student, College of Mechanical Engineering, Zhejiang University of Technology, Hangzhou, China

ABSTRACT

The global and local limit loads of nozzle corner cracks in a typical reactor pressure vessel (RPV) are investigated under combined loading including internal pressure, nozzle axial force and nozzle bending moment using elastic-plastic finite element (FE) method. Several estimation approaches are compared with the FE results. For global limit load solution, the parabolic function can predict a conservative result. However, the related error will exceed 50% under the bending moment. The J-integral values of different models for local limit load solutions are compared, including the API 579 and EPRI approaches, as well as the plate model with a through-wall crack. The plate model solution is the closest to R6 OPT-2 in the conservative case to predict the *J* value. It is suggested to use the plate model with a through-wall crack to further modify and predict the local limit load of nozzle corner crack under combined loading.

INTRODUCTION

The structural integrity of nuclear power plant components is the basis for the safe operation of nuclear power plants. However, small cracks, such as nozzle corner cracks, are frequently discovered during operation in engineering practice due to the cyclic loading. Structural integrity assessment of the defective components is usually required if the defects cannot be repaired. The *J*-based failure assessment diagram (FAD) method is widely applied for structural integrity assessment, which has been adopted in most fitness for service standards or codes, such as R6 (2019), BS 7910 (2019), API 579 (2016). In the *J*-based FAD method, the elastic-plastic fracture parameter, *J*, is estimated via the limit load and elastic *J*, or, equivalently, the stress intensity factor (SIF)(1984). For nozzle corner cracks, the SIF solutions are normally provided in part of the structural integrity assessment procedures/standards. However, the corresponding limit load solutions consider in most of these procedures/standards only consider internal pressure, while the combined load solutions required for the evaluation of engineering structural integrity are sometimes not available and need to be developed.

The common tee in pressure vessels has a similar external shape to the nozzle structure. From a geometrical perspective, the intersection of two cylinders is a shared feature between the tee and the nozzle of vessels. The difference lies in the larger diameter of the two cylinders in the tee. Therefore, the limit load analysis of the two structures is similar. For the limit load of the nozzle component, Lee et al. (2015) proposed solutions for the limit pressure and bending moment of the tee structure around the intersection without any welding or reinforcement, based on FE calculations. Xuan et al. (2006) derived estimation formulas for the limit load of defect-free tees under internal pressure and bending moment loads. Regarding the corner crack component of the nozzle, Xuan et al. (2003) studied the failure process and failure characteristics of defect-free and cracked tee, summarizing the variation law of the plastic limit load of defect-free tees with structural dimensions and the weakening effect of cracks on the limit load. Chen et al. (2010) proposed the use of the modified elastic compensation method, elastic compensation method, and elastic-plastic analysis method to calculate the plastic limit load of thin-walled tee junctions with angled cracks under internal pressure. Apart from that, there is limited research on the

limit load of corner crack nozzle structures under complex loading conditions. In this paper, the influence of combined loading on the limit load of nozzle structure is studied, including internal pressure load and external load. The limit load solution under combined loading should be established.

The layout of this article is as follows. Section 2 defines the geometric parameters and normalization of the limit load. Section 3 describes a global/local limit load solution for nozzle corner cracks. Section 4 describes the details of elastic-fully plastic FE analysis. Section 5 summarizes and discusses solutions to limit loads, and Section 6 gives conclusions.

DEFINITIONS OF GEOMETRY AND LOADING PARAMETERS

In this paper, the inner corner cracks of the nozzle in a reactor pressure vessel is studied. Figure 1 shows the geometry of the inner corner of the nozzle with a crack defect. Where R_m and R_n are the inner radius of the RPV cylinder and the nozzle, t and t_n are the wall thickness of the cylinder and the connector, and a is the crack depth of the corner semi-ellipse. In order to facilitate expression and applicability of the results, these parameters are normalised, including dimensionless crack depth α, crack size φ, ratio of cylinder thickness to cylinder mean radius κ, ratio of cylinder thickness to nozzle thickness δ, ratio of nozzle radius to cylinder mean radius γ as follows.

$$\alpha = \frac{a}{t}, \quad \varphi = \frac{a}{c} \tag{1}$$

$$\kappa = \frac{t}{R_m}, \quad \delta = \frac{t}{t_n}, \quad \gamma = \frac{R_n}{R_m} \tag{2}$$

The combined loading considered in this paper includes the internal pressure p, which acts jointly with the external load of the nozzle. The external load of the nozzle includes the axial tension/compression force N acting on the end face of the nozzle and the bending moment M_x/M_y acting on the whole nozzle. The applied and positive and negative directions are shown in Figure 2. The limit load corresponding to internal pressure p, to axial force N and bending moment M is expressed by p_L, N_L and M_L respectively. For combined loading, the load ratios λ_1 and λ_2 are defined as:

$$\lambda_1 = \frac{N}{\pi R_n^2 p} \tag{3}$$

$$\lambda_2 = \frac{M}{R_a \pi R_n^2 p} \tag{4}$$

Where, R_a is the mean radius of the nozzle with $R_a = R_n + \frac{t_n}{2}$.

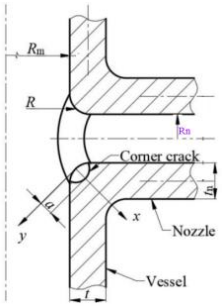

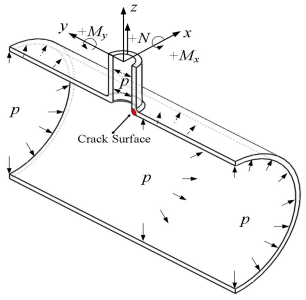

Figure 1. Nozzle corner structure with surface cracks

Figure 2. Loading diagram of the nozzle cylinder members with corner cracks

LIMIT LOAD SOLUTION

In this section, the limit load scheme of nozzle corner crack under internal pressure in existing standard is introduced, and a new limit load estimation method is obtained by simplifying the nozzle corner model with reference to the through-wall crack plate model.

Global Limit Load Solution

The local limit load of the cracked component generally corresponds to the load level of the cracked ligament or the local region where the plastic yield occurs, which may be related to the fracture of the cracked local small ligament. The global limit load corresponds to the load when all the ligaments of the crack enter plastic yield, which is physically calculated by the load of the structure and the displacement behavior of the load point. According to the existing research results, based on the superposition law of linear equation (Equation 5), parabolic equation (Equation 6) or elliptic equation (Equation 7), based on the limit load of the member under single load, the whole limit load of the cracked member under complex load is predicted. According to the loading conditions of different complex loads, the limit load superposition law of cracked components can be expressed as:

$$\frac{p_L}{p_L^*}+\frac{N_L}{N_L^*}=1,\ \ \frac{p_L}{p_L^*}+\frac{M_L}{M_L^*}=1 \tag{5}$$

$$\left(\frac{p_L}{p_L^*}\right)^2+\frac{N_L}{N_L^*}=1,\ \left(\frac{p_L}{p_L^*}\right)^2+\frac{M_L}{M_L^*}=1 \tag{6}$$

$$\left(\frac{p_L}{p_L^*}\right)^2+\left(\frac{N_L}{N_L^*}\right)^2+\left(\frac{M_L}{M_L^*}\right)^2=1 \tag{7}$$

Where p_L, N_L and M_L represent the corresponding limit load under combined loading, and p_L^*, N_L^* and M_L^* represent the corresponding limit load of the structure under a single loading.

Local Limit Load Solution Based on the Nozzle Reinforcement Range

Considering the reinforcing effect of the nozzle on the cylinder, the corner crack can be regarded as a hole edge corner crack plate considering the reinforcement range modification. It defines the reference stress of the structure in terms of the area reduction caused by the crack in the reinforcement zone, as shown in Equation 8.

$$\sigma_{\text{ref}}=P_{\text{m}}\left(\frac{2.5t_n^2+\left(q-R_n\right)t}{2.5t_n^2+\left(q-R_n\right)t-0.25\pi a^2}\right) \tag{8}$$

Where, P_{m} is the primary member stress at the corner of the nozzle; q is the nozzle reinforcement region size. The definition is as follows:

$$q=\max\left\{2r_n,\left(r_n+t_n+t\right)\right\} \tag{9}$$

$$P(x) = P_0 + P_1\left(\frac{x}{t}\right) + P_2\left(\frac{x}{t}\right)^2 + P_3\left(\frac{x}{t}\right)^3 + P_4\left(\frac{x}{t}\right)^4 \tag{10}$$

$$P_m = P_0 + \frac{P_1}{2} + \frac{P_2}{3} + \frac{P_3}{4} + \frac{P_4}{5} \tag{11}$$

From this, the limit load solution P_L of the corner crack structure with nozzle in API 579 (2016) can be obtained under the action of internal pressure P_L. Where P_l is the applied primary load, such as the internal pressure load p.

$$P_L = \left(\frac{\sigma_0}{\sigma_{ref}}\right) P_l \tag{12}$$

Local Limit Load Solution Based on the Plate Model with Hole Corner Crack

EPRI Method 1

EPRI (1981) proposed the limit load solution of corner crack simulated by a plate with a central hole and a single radial crack. As shown in Figure 3, the plate is $2b$ wide and contains a hole of radius R and a radial crack of length a. It is subjected to a uniform stress distribution of is in the y direction and is in the x direction. Considering the reduction of the area of the net cross-section, the corresponding limit load can be defined as:

$$\sigma_L^{\infty} = \frac{\sqrt{3}}{2}\frac{(2b - 2R - a)\sigma_0}{2b} \tag{13}$$

EPRI Method 2

Further, simplification was carried out in subsequent EPRI updates. When the reference stress range is about 10 times the crack half-length, the simplified limit load solution can be obtained immediately:

$$\sigma_L = 1.0952\left[1 - 0.08696\left(1 + 0.5\frac{a}{R}\right)\right] \tag{14}$$

Local Limit Load Solution Based on the Crack Plate Model

In the case of pure internal pressure, the nozzle part can be ignored when the radius of the cylinder is large enough. The whole nozzle opening can be regarded as a part of the crack, and it is regarded as a flat plate with through-wall crack. In this case, the crack half-length can be regarded as r_n+a. Under internal pressure load, the model can be simplified to a plate model with penetrating cracks under biaxial load. Referring to the limit load solution of Lei(2015) surface cracked plate under biaxial load Figure 4, it is simplified to the limit load of penetrating cracked plate under multi-axial load(plate solution), which can be expressed as:

$$n_L = \frac{1 - \beta}{\sqrt{1 - \lambda(1 - \beta) + [\lambda(1 - \beta)]^2}} \tag{15}$$

Where, $\beta = \frac{c}{W}$, $\lambda = \frac{\sigma_x}{\sigma_m}$, W is the width of the plate, t is the thickness of the plate, and $2c$ is the crack length.

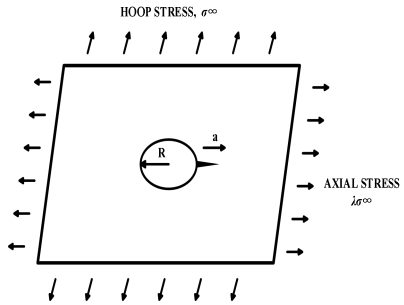

Figure 3. Two-dimensional plate model of nozzle corner crack

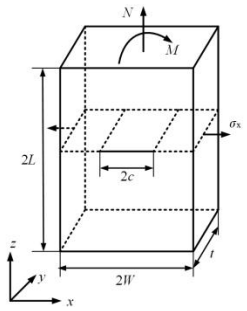

Figure 4. Surface crack plate model under multi-axial load

FE ANALYSIS

Elastoplastic FE analysis of nozzle with elliptic cracks on inner surface corner was carried out under internal pressure and external nozzle load (including axial tension/compression force and overall bending moment) alone or combined to verify the global and local limit load solutions. The analysis was performed using ABAQUS 2018 version.

Geometries and Crack Model

A three-dimensional FE model was established and analysed to validate the estimated limit load solutions. The structural model used in the analysis is characterized by a cylindrical body with an internal radius of 2130 mm. The schematic representation of the model structure is shown in Figure 1. The analysis parameters are summarized in Table 1.

Due to the symmetry of geometry and loading conditions, 1/4 and 1/2 of the RPV nozzle model are used respectively. The 1/4 model is used to study the influence of internal pressure and axial tension/compression stress on the limit load under single or combined loading, while the 1/2 model is used to consider the presence of the nozzle bending moment. The direction and positivity of the external load on the nozzle are defined in Figure 2.

Table 1. Structural parameters of nozzle corner crack

Dimensionless Parameter	κ	δ	γ	α	φ
Parameter Values	0.0705, 0.141	1.0, 1.5	0.1	0.02, 0.05, 0.1, 0.2, 0.5	0.333, 1.0

FE Meshes

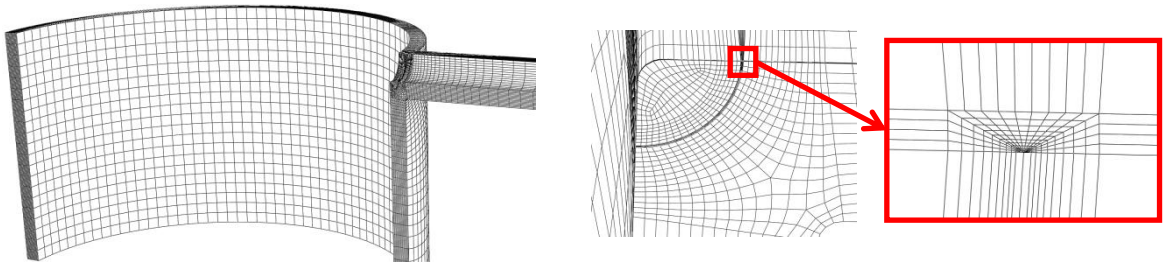

(a)Global mesh (b)Local mesh

Figure 5. A typical FE mesh for κ=0.0705, δ=1.0, γ=0.1, φ=1.0, a/t=0.2

The ABAQUS FE model uses 8-node hexahedron element in the overall model and 8-node collapse wedge element in the crack tip. Focused mesh is employed around the crack tip which is good for the calculation of stress intensity factor (SIF) and J integral in further study but can also be used in the limit load analyses.

Material Properties

For limit load analyses, an idealised elastic-perfectly plastic stress- strain relationship is used with Young′ s modulus E=204000MPa, Poisson's ratio ν=0.3, and yield strength σ_y=345MPa.

Definitions of Global and Local Limit Loads

The elastic-perfectly plastic FE analysis does not directly give the limit load and further post-processing and judgement should be used to determine the load value at plastic collapse. In this paper, the twice elastic slope (TES) method recommended by ASME (2021) is adopted to determine the FE global limit loads.

The FE local limit load is defined as the crack ligament yielding. The FE results are observed to check the Von Mises stress compared with the yield stress in the crack ligament. Figure 6(b) shows an example to determine the local limit load. When the plastic zone penetrates the small ligament, the corresponding LPF is used to determine the local limit load.

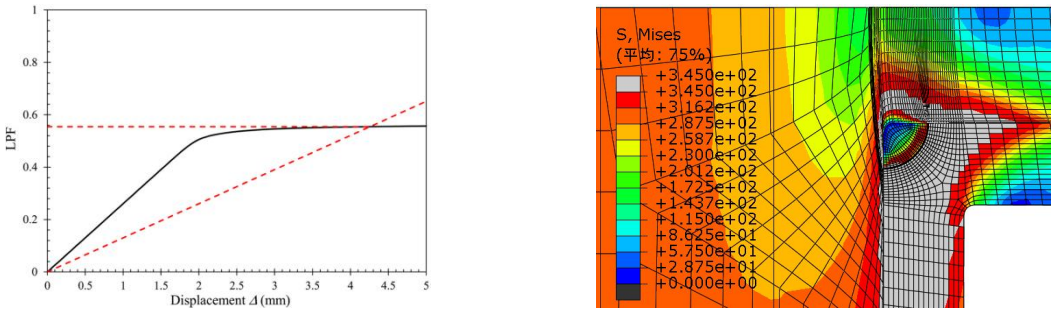

(a)LPF vs. displacement at the reference point (b)LPF=0.55

Figure 6. (a)The global limit load is determined by double slope method(b)Determination of the local limit load from Von Mises stress distribution(κ=0.0705, δ=1.0, γ=0.1, φ=1.0, a/t=0.2)

J ESTIMATION BASED ON THE REFERENCE STRESS METHOD

In the reference stress J scheme (2015), the ratio between the total J and the elastic J_e, can be estimated from the following equation based on the R6 Option 2 FAC (2019):

$$\frac{J}{J_e} = \frac{E\varepsilon_{ref}}{\sigma_{ref}} + \frac{L_r^2}{2}\frac{\sigma_{ref}}{E\varepsilon_{ref}} \tag{16}$$

Where, σ_{ref} represents the reference stress and ε_{ref} represents the reference strain determined by the reference stress and stress-strain relationship. L_r represents the load ratio, indicating the degree to which the load is close to the plastic yield limit load. L_r can be determined by the following formula:

$$L_r = \frac{\sigma_{ref}}{\sigma_y} = \frac{P}{P_L} \tag{17}$$

where P is the applied primary load, in general, and P_L is the limit load corresponding to the load type P for the cracked structure and σ_y is the yield stress or 0.2% proof stress for the material considered. Equation 17 also defines the relationship between the reference stress for the given load and limit load.

RESULTS AND DISCUSSION

Influence of Axial Force and Bending Moment Applied Direction on Limit Load

Figure 7 shows the combined loading of internal pressure p(MPa), nozzle axial force N(N) and nozzle bending moment M_x(N·mm). According to the FE results, the positive and negative of the M_x direction of the bending moment load has no effect on the limit load of the crack member at the corner of the nozzle. Therefore, the estimated value of the bending moment load in the negative direction can be considered as the positive direction for the estimation of the limit load when considering the bending moment. The positive and negative axial force in the direction N of the nozzle has a certain influence on the limit load of the member. When the axial load of the nozzle is tensile load, the bearing capacity of the cracked member will be reduced. As can be seen from Figure 7, when the external load of the nozzle is small, the limit load value will increase. However, as the nozzle load increases, the limit load value will continue to decrease. This is because the nozzle axial compression load will partially offset the balance load caused by the internal pressure, but with the increase of the nozzle load, the nozzle load dominates, resulting in a decrease in the limit load.

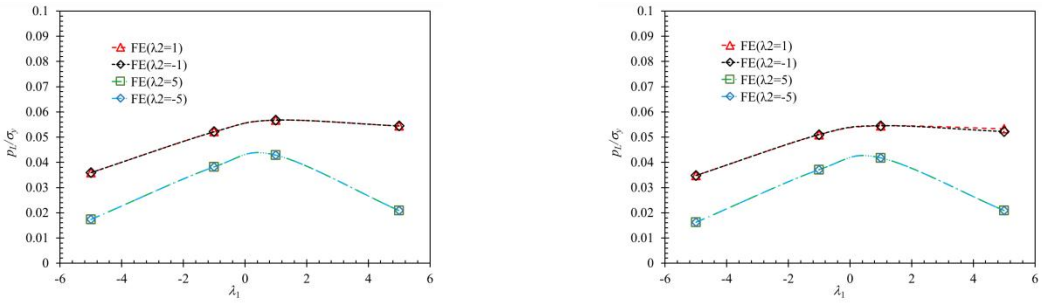

(a) a/t=0.02 (b) a/t=0.2

Figure 7. FE solution of limit load of member under joint load (κ=0.0705, δ=1.5, γ=0.1, φ=1.0, *p, N,* M_x combined loading)

Limit Load Verification

Global Limit Load

Based on the corresponding superposition law, the estimated global limit load of the pipe with corner crack under complex load is calculated and compared with the FE value calculated by the double elastic slope method. Figure 8 (a) shows the combined loading of p and N. When the axial force of the nozzle is positive (pressure), the linear equation (Equation 5) can accurately and conservatively estimate the overall limit load. When the axial force of the nozzle is negative (pull), the parabolic equation (Equation 7) can accurately and conservatively estimate the overall limit load. Figure 8 (b) shows the combined loading of p and M_x. It can be seen that the parabolic equation (Equation 7) can conservatively estimate the overall limit load. However, when the load is relatively large and the bending moment load is the dominant factor, the prediction result of the parabolic equation is conservative but the error is large, while the elliptic equation Equation 8 can accurately estimate the overall limit load. Figure 8 (c) shows that under the combined loading of P, N and M_x, the parabolic equation (Equation 7) can conservatively estimate the overall limit load. When internal pressure and nozzle axial force load dominate, the prediction results of the parabolic equation are conservative and the error is small. When the bending moment load dominates the parabolic equation, it exhibits a significant error in predicting the global limit load, while the elliptic equation can accurately predict it in this case.

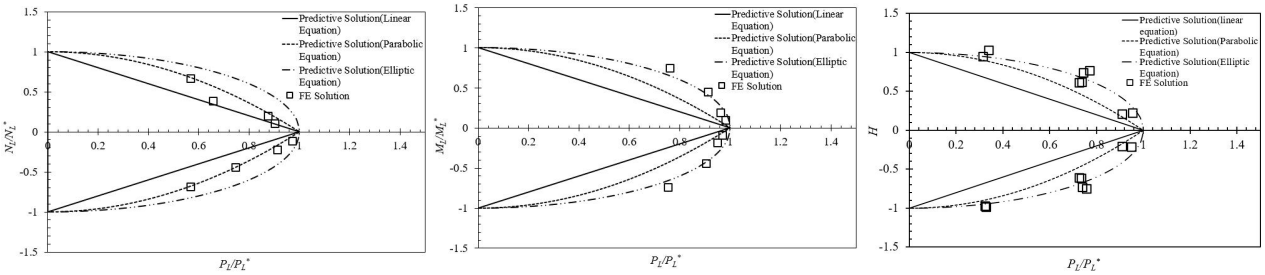

(a) (b) (c)

Figure 8. Comparison of global limit load prediction solution and FE solution (κ=0.0705, δ=1.5, γ=0.1, φ=1.0, α=0.05) (a) p and N combined loading, (λ_2=0; λ_1=1,2,5,10,-1,-2,-5,-10); (b) p and M_x combined loading, (λ_1=0; λ_2=1,2,5,10,-1,-2,-5,-10); (c) p, N, M_x combined loading, (λ_1、$_2$=±1,±5, $H = \sqrt{\left(N_L / N_L^*\right)^2 + \left(M_L / M_L^*\right)^2}$)

Comparison of Local Limit Load Models

Figure 8 and Figure 9 compare the J/Je values under different crack depths, cylinder and nozzle thicknesses under internal pressure loads. It can be seen from the figure that the J-integral estimated by EPRI, API 579 method or the limit load solution based on the through-wall crack Plate model (plate curve in the figure) is lower than the predicted value of the R6 OPT-2. This shows that more conservative results can be obtained by using these local limit loads in defect assessment. From the perspective of conservative degree, API 579 method is too conservative, EPRI method is second, Plate curve is closest to R6 OPT-2.

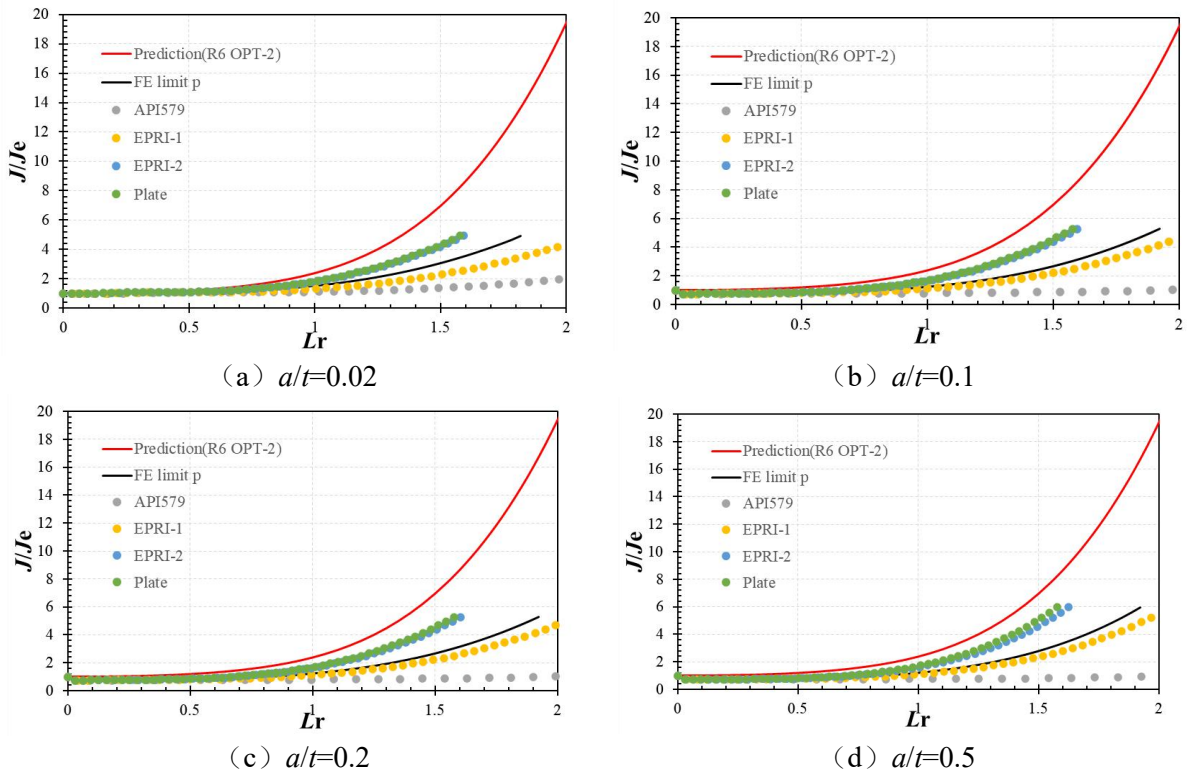

（a）a/t=0.02　（b）a/t=0.1

（c）a/t=0.2　（d）a/t=0.5

Figure 8. Comparison of J/J_e values and finite element values of different models under internal pressure loads (a/c=1,t/R_m=0.0705, δ=1.5)

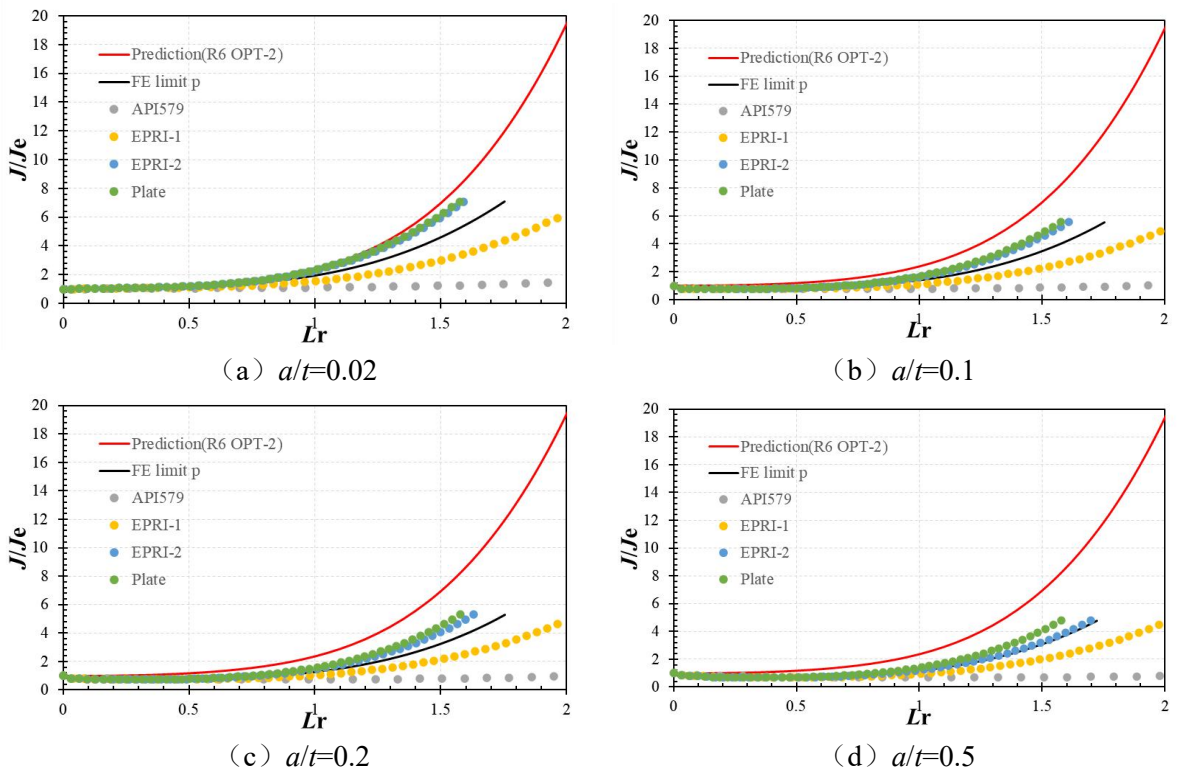

（a）a/t=0.02　（b）a/t=0.1

（c）a/t=0.2　（d）a/t=0.5

Figure 9. Comparison of J/J_e values and finite element values of different models under internal pressure loads (a/c=1,t/R_m=0.141, δ=1.5)

CONCLUSIONS

Elastoplastic FE method is used to study the global and local limit loads of the nozzle with elliptical corner cracks under the combined loading including internal pressure, nozzle axial force and nozzle bending moment. According to the global limit load, the linear equation can conservatively predict the *pN* combined load, and the parabolic equation can conservatively predict the combined load of pM_x and pNM_x. What's more, when the bending moment load dominates the parabolic equation, it exhibits a significant error in predicting the global limit load, while the elliptic equation can accurately predict it in this case.

For the local limit load model, the Plate solution is the closest to R6 OPT-2 to predict J value in the conservative case by J integral comparison analysis. It is suggested to use the plate model with a through-wall crack to further modify and predict the local limit load of nozzle corner crack under complex load.

REFERENCES

API 579-1/ASME FFS-1. (2016). *Fitness-For-Service 2016*, the American Petroleum Institute and the American Society of Mechanical Engineers.

Ainsworth, R. A. (1984). "The assessment of defects in structures of strain hardening material". *Engineering Fracture Mechanics*, 19(4), 633-642.

BS7910. (2019). *Guide to Methods for Assessing the Acceptability of Flaws in Metallic Structures*, BSI Standards Publication.

Chen, L., Liu, Y., & Gang, T. (2010, May). "Plastic limit load analysis of tee joint containing corner cracks". *In AIP Conference Proceedings (Vol. 1233, No. 1, pp. 316-321)*. American Institute of Physics.

Design. (2021). ASME Boiler and Pressure Vessel Code, Section III, Rules for Construction of Nuclear Facility Components, American Society of Mechanical Engineers, New York.

Kumar V, German M. D. ,Shih C. F. (1981). "An Engineering Approach for Elastic-Piastic Fracture Analysis", *Eiectric Power Research Institute.*

Lei, Y., & Budden, P. (2015). "Global limit load solutions for plates with surface cracks under combined biaxial forces and cross-thickness bending", *International Journal of Pressure Vessels and Piping*, 132, 10-26.

Lee, K. H., Kim, Y. J., Budden, P. J., & Nikbin, K. (2009). "Plastic limit loads for thick-walled branch junctions". *The Journal of Strain Analysis for Engineering Design*, 44(2), 143-148.

R6. (2019). *Assessment of the Integrity of Structures Containing Defects*, Revision 4, Amendment 12, EDF Energy Nuclear Generation Ltd., Gloucester, UK.

Xuan F Z, Li P N, Tu S T. (2006). "Limit load analysis for the piping branch junctions under in-plane moment". *International Journal of Mechanical Sciences*, 48(4): 460-467.

Xuan F Z, Hui H, Huang Z H, et al. (2003). "Study on Plastic Limit Load of extruded Tee under Internal Pressure ". *Pressure Vessels*, 2003(01): 1-32.